Manipulation of Planar Oxygen Defect Arrangements in Multifunctional Magnèli Titanium Oxide Hybrid Systems: From Energy Conversion to Water Treatment

Yichen Liu, Jack Yang[a], Yang Liu, Jian Zheng, Wen Lee, Junjie Shi, Jonathan Horlyck, Jiangzhou Xie, Yee Yan Tay, Thiam Teck Tan, Dehong Yu, Richard Mole, Garry McIntyre, Changyong Zhang, Cui Ying Toe, T. David Waite, Jason Scott, Yu Wang, Tom Wu, Shenghao Han and Sean Li

Supplementary Information

Table S1 Reported room temperature electrical and thermal properties of titanium oxides with general formula Ti_nO_{2n-1} and their mother structure TiO_2. The layer thickness in the table 1 is defined and calculated as the distance between each interfaces/shear plane (the yellow lines) in Figure 1 (a).

Ti_nO_{2n-1} phase	***Space group***	***Layer thickness (nm)***	***Electrical conductivity (σ/S cm^{-1})***	***Thermal conductivity (W/m·K)***	***Phonon thermal conductivity (W/m·K)***	***Thermoelectric***	***Photothermal***	***Catalytic***
Ti	$P4_2/mnm$, hexagonal	n/a	2000 [19]	~20 [19]	No record	No record	No record	Yes
Ti_2O_3	$R\bar{3}c$,trigonal	0.2592nm	1052 [16]	3.7 [16]	2.9 [16]	Yes	Yes	Yes
Ti_3O_5	$C2/c$, monoclinic	0.3741nm	630 [15]	No record	No record	No record	No record	Yes
Ti_4O_7	$P\bar{1}$, triclinic	0.5162nm	1035 [17]	~3.5 [17]	~2.7 [17]	Yes	No record	No record
Ti_5O_9	$P\bar{1}$, triclinic	0.7776nm	450 [18]	~2.2 [18]	~2.1 [18]	Yes	No record	No record
Ti_6O_{11}	$P\bar{1}$, triclinic	1.0898nm	63 [15]	~2.1 [15]	~2 [15]	Yes	No record	No record
Ti_7O_{13}	$P\bar{1}$, triclinic	1.1445nm	No record	2.5 [14]	2 [14]	Yes	No record	No record
Ti_8O_{15}	$P\bar{1}$, triclinic	1.1745nm	25 [15]	2.5 [14]	2.0 [14]	Yes	No record	No record
Ti_9O_{17}	$P\bar{1}$, triclinic	1.4192nm	18 [15]	~2 [15]	~1.98 [15]	Yes	No record	No record
TiO_2	$P4_2/mnm$, tetragonal	n/a	~16 [20]	~3 [20]	~2.98 [20]	Yes	Yes	Yes

Table S2 The ICCD information used during the Rietveld analysis.

Phase	Ti_2O_3	Ti_3O_5-1	Ti_3O_5-2	Ti_2O-1	Ti_2O-2	TiO
Crystal system	Rhom $R\bar{3}c$ (167)	Mono $C2/m$ (12)	Mono $C2/m$ (12)	Hex $P3m$ (164)	Hex $P6/3m$ (191)	$Fm3m$ (225)
$a(\text{Å})$	5.1489	9.74	9.8261	2.96	4.9915	4.2930
$b(\text{Å})$	5.1489	3.8	3.7894	2.96	4.9915	4.2930
$c(\text{Å})$	13.6427	9.44	9.9694	4.83	2.8794	4.2930
α	90	90	90	90	90	90
β	90	91.5	91.258	90	90	90
γ	120	90	90	120	120	90
Ti content (*wt%)*	66.62	64.24	64.24	85.69	85.69	74.96
ICCD	04-005-4632	04-008-1596	04-007-6635	04-005-4375	04-007-2361	04-016-4319

Table S3 The quality of the refinement results.

Sample	R_B						R_{exp}	R_{wp}	*GOF*
	Ti_2O_3	Ti_3O_5-1	Ti_3O_5-2	Ti_2O-1	Ti_2O-2	TiO			
71.6%Ti_2O_3-28.4%Ti_3O_5	3.41	4.04	3.02	-	-	-	2.11	5.86	2.77
70.3%Ti_2O_3-29.3%Ti_3O_5-0.5%TiO	3.94	4.01	3.42	-	-	3.02	2.15	6.54	3.03
62.7%Ti_2O_3-35.8%Ti_3O_5-1.5%Ti_xO	3.9	4.12	3.43	-	1.78	2.8	2.19	6.46	2.94
47.8%Ti_2O_3-48.3%Ti_3O_5-3.9%Ti_xO	4.52	4.82	5.76	6.91	1.48	4.4	2.16	8.12	3.75

Table S4 The setting parameters for operations on Lambda 950

Parameter setting		
Scanning Range		380-1100nm
Scanning Intervals/speed		4nm
Monochromator		860.80nm
CBM		100%
Slit	PMT	2nm
	Pbs	2nm
CBD		selected
Detector Change		860.80nm

Table S5. Band positions of all the samples

	E_v	E_c	***Bandgap***
71.6%Ti_2O_3-28.4%Ti_3O_5	2.91 eV	1.29 eV	1.62 eV
70.3%Ti_2O_3-29.3%Ti_3O_5-0.5%TiO	2.86 eV	1.33 eV	1.53 eV
62.7%Ti_2O_3-35.8%Ti_3O_5-1.5%Ti_xO	2.83 eV	1.37 eV	1.46 eV
47.8%Ti_2O_3-48.3Ti_3O_5-3.9%Ti_xO	3.02 eV	1.66 eV	1.36 eV

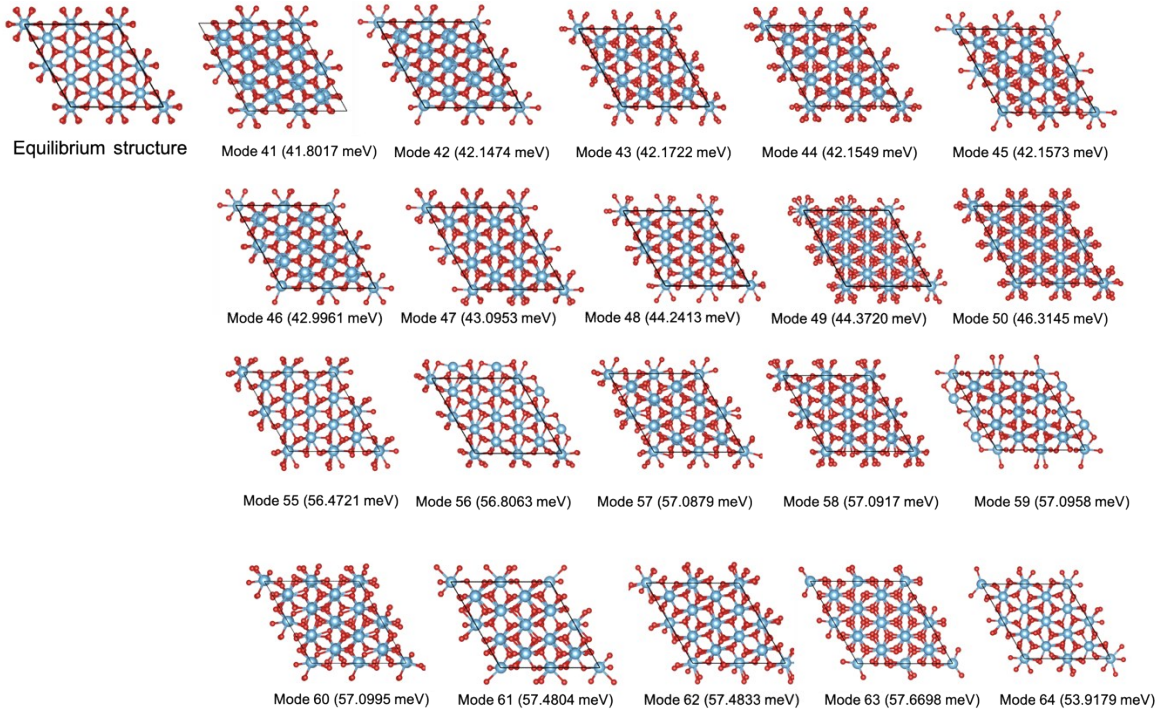

Figure S1 Examples of phonon-mode-modulated structures of Ti_2O_3 along the Γ-point eigenvectors with dominant contributions from the vibrations of oxygen-sublattices.

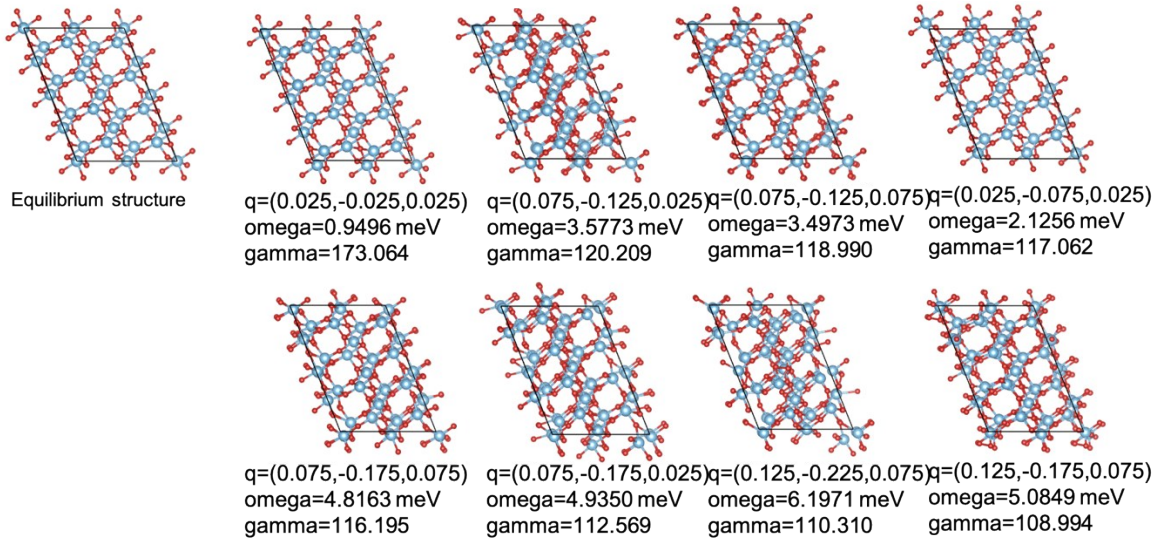

Figure S2 Examples of phonon-mode-modulated structures of Ti_3O_5 along phonon modes with largest Grüneisen parameters (γ).

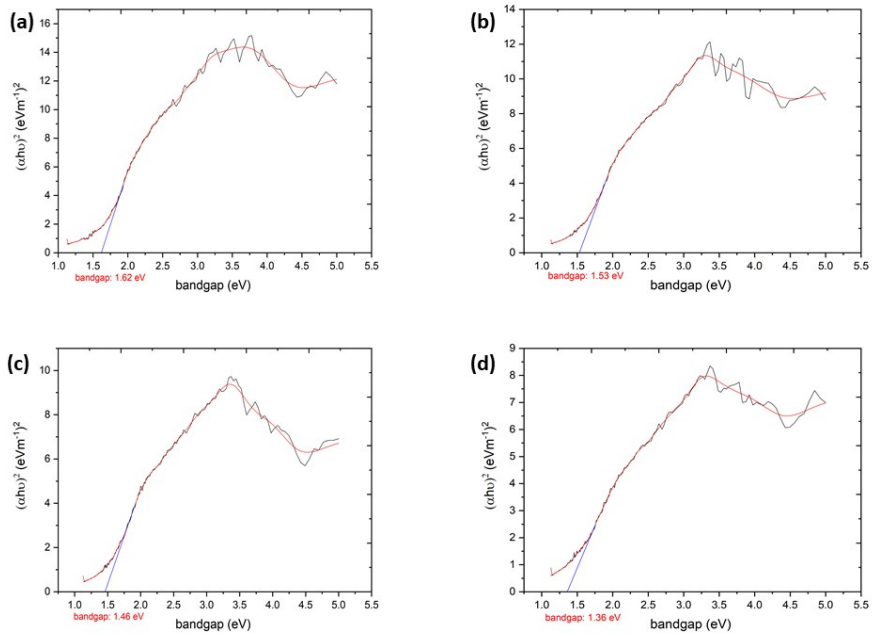

Figure S3 The bandgap calculations of all the samples using Kubelka-Munk function

Calculation of Band gap using Tauc Plot

For the band gap calculation, the following relational expression proposed by Tauc,Davis, and Mott is used.

$$(h\nu\alpha)^{1/n} = A(h\nu - E_g)$$

Where:

The Planks constant (h) =4.1357*10^{-15} ev·s, frequency of vibration (ν) = the speed of light in vacuum(c) / the photon's wavelength(λ), α is absorption coefficient, E_g represent the band gap, A is proportional constant. n is determined to be 1/2. (n = 2 for an indirect allowed transition; n = 3 for an indirect forbidden transition; n = 1/2 for a direct allowed transition; n = 3/2 for a direct forbidden transition.)

Here we use $BaSO_4$ as reference sample, the relatively diffuse reflectance can be obtained by $R_d=R_{Ti}/R_{Ba}$*100%.

The absorption coefficient was calculated by the following equation:

α=log($1/R_d$)

The $(\alpha h\nu)^2$ on the horizontal axis was plotted against the hν.

A line is drawn tangent to the point of inflection on the curve of $(\alpha h\nu)^2$vs hν, and the hν value at the point of intersection of the tangent line and the horizontal axis is the band gap E_g value.

Note: The point of inflection is found by taking the first derivative of the curve. The point at which the value of the first derivative coefficient begins to decrease after increasing is the point of inflection.

Calculation of Solar-absorption efficiency

Our sample thickness is around 3.1mm, thus the light(280-1100nm) transmitted through the sample is neglect. Then we have absorption $A=1-R_d$. The combination of the standard Air Mass 1.5 solar spectra (ASTM G-173-03) and the absorption spectra gave the solar absorption of our sample in different spectrum region. The results can be calculated via:

Solar absorption = Solar Spectral irradiance * Absorption

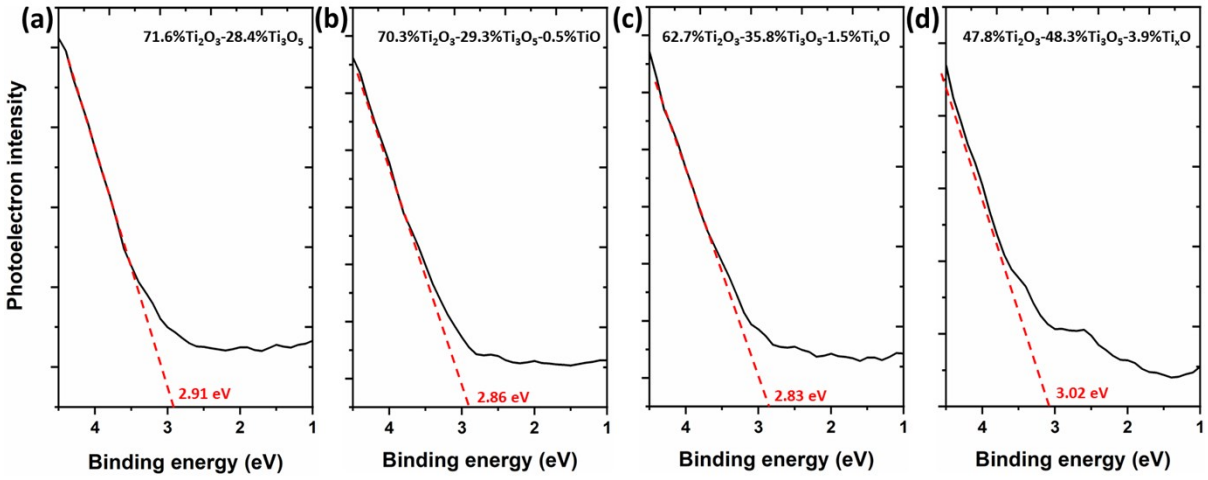

Figure S4. The valence band spectrum measured by UPS.